

## High Resolution Analysis of CRM 137A via Decay Energy Spectroscopy

R. Schönemann<sup>1</sup>, M. P. Croce<sup>1</sup>, K. A. Schreiber<sup>1</sup>, M. H. Carpenter<sup>1</sup>, D. R. Schmidt<sup>2</sup>, J. N. Ullom<sup>2,3</sup>, K. J. Mathew<sup>1</sup>

- 1) Los Alamos National Laboratory, Los Alamos, NM, USA
- 2) National Institute of Standards and Technology, Boulder, CO, USA
- 3) University of Colorado, Boulder, CO, USA

### INTRODUCTION

Nuclear reference materials are essential in providing an exact standard for quality control and instrument calibration. This work is part of an ongoing effort to recertify the plutonium reference material CRM 137A, which is currently awaiting review and value assignment from multiple laboratories and methods. Measurements of Pu isotopic ratios are essential in safeguards, nonproliferation and nuclear forensics, where they can provide information about the origin and processing history of the nuclear material. Traditional methods for isotopic analysis are mass spectrometry and  $\alpha$ -spectroscopy. Mass spectrometry is a powerful tool that can achieve high accuracies, drawbacks include the cost and complexity of the instrument and sample preparation requirements. On the other hand,  $\alpha$ -spectroscopy with Si-detectors is simple and inexpensive but requires careful sample preparation to achieve thin deposits of nuclear material to avoid line broadening due to energy absorption in the source. Typical energy resolutions for  $\alpha$ -spectroscopy range about 10keV fwhm (full width half maximum) and might not be able to separate nearby close  $\alpha$ -energy lines. Here we present results of Pu isotopics of CRM 137A via Decay Energy Spectroscopy (DES) which overcomes many of the limitations faced by other techniques.

### DECAY ENERGY SPECTROSCOPY

DES is a technique where the nuclear material is embedded into a gold absorber, which is thermally coupled to a superconducting Transition Edge Sensor (TES) [Koehler2013, Hoover2015]. Here, the TES is a Mo/Cu bilayer thin film biased at its superconducting transition and operated at a temperature of 80mK [Irwin2005]. Thus, a small increase of the temperature, induced by a nuclear decay in the absorber, leads to a measurable change in the TES resistance, which is translated into a voltage pulse and recorded with the data acquisition software. A schematic of a typical microcalorimeter DES-type detector based on a 5mm x 5mm Si chip is shown in Figure 1. The gold absorber is indium bonded to a mounting pad next to the TES. Both are located on the central island of the chip (see photos in Figure 1), which is connected to the frame by meandering Si paths providing a thermal link between the island and the thermal bath. The length of the meandering paths can be altered to adjust the thermal conductivity between the Absorber/TES and the bath - allowing for different sized absorbers and detectable energy ranges.

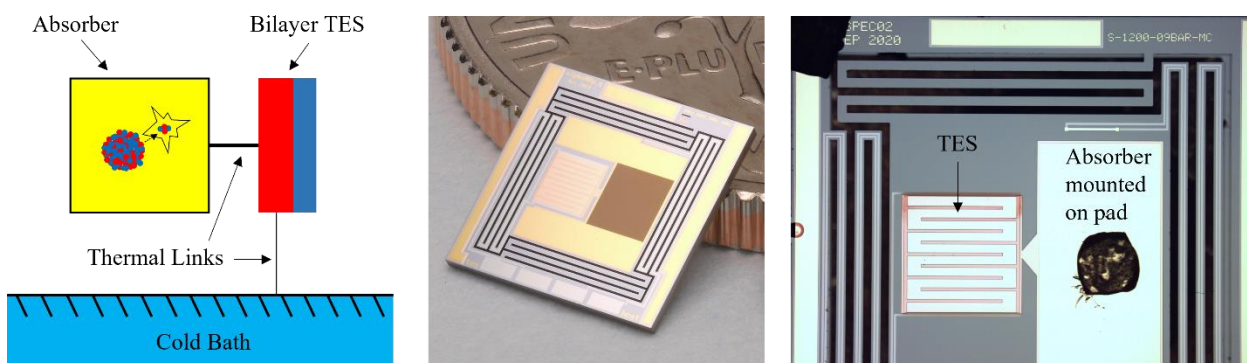


Figure 1: (Left) Schematic of TES detector pixel showing functional components. Each of the labeled components may be adjusted to change the performance characteristics of the detector. (Center) Photo of DES-type chip propped on a United States dime for scale. (Right) Close-up of DES-type chip die with mounted sample. The TES is offset and thermally linked to an absorber on a thermally isolated island, with meandering thermal links to the outside of the chip anchored to the thermal bath.

The detectors are operated in a pulse tube cooled cryostat equipped with an adiabatic demagnetization stage that allows for 8 detectors to be measured simultaneously and can achieve 12h hold times at 80mK before it undergoes a 2h regeneration cycle.

In general, DES measures the total amount of energy released during a nuclear decay (Q-value) which includes the energy of the  $\alpha$ -particle ( $\sim 5\text{MeV}$ ), the recoiling daughter nucleus ( $\sim 100\text{keV}$ ), electrons and  $\gamma$ /X-rays ( $< 20\text{keV}$ ). The decay products thermalize via interactions with the Au lattice and, in the case of Pu, produce a single energy peak for each isotope regardless of the exact decay path (see Figure 2). A gold absorber thickness of  $15\mu\text{m}$  is sufficient to stop all radiation for the relevant Pu decay chains. Higher energy  $\gamma$ -rays associated with Pu  $\alpha$ -decays have small enough branching ratios that they can be neglected.

## SAMPLE PREPARATION

Three DES samples of CRM 137A (1A, 1B, 1C), each with an activity of about 1Bq, were prepared by pipetting  $1\mu\text{L}$  Pu(IV) nitrate solutions on  $25\mu\text{m} \times 1.5\text{mm} \times 1.5\text{mm}$  sized gold foils and air dried. The size of the absorber was chosen to achieve a total heat capacity of  $\sim 400\text{pJ/K}$  at 100mK for optimal detector performance at 5MeV. The absorber was folded and mechanically kneaded with pliers for 100 cycles as described in [Hoover2015]. This treatment significantly reduces low energy tailing and improves energy resolution. During the kneading process the Pu(IV) nitrate residue is broken up and incorporated in the gold matrix, therefore the  $\alpha$ -particles deposit their energy in the gold rather than the Pu(IV) nitrate residue. Presumably, this avoids peak broadening due to differences in lattice damage effects and thermal properties between the gold matrix and Pu(IV) nitrate residue.

The absorber was bonded to the mounting pad next to the TES with a small piece of indium. A picture of the mounted absorber on the detector chip is shown in Figure 1.

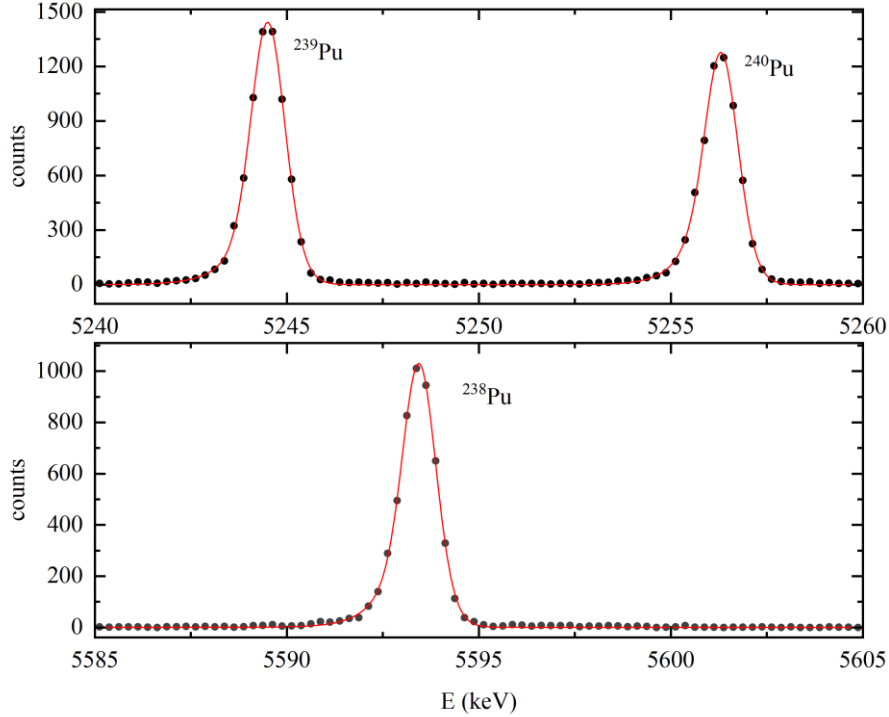


Figure 2: *Q*-value spectrum for sample 1B (run number 3) showing the counts per 250eV bin for  $^{239}\text{Pu}$ ,  $^{240}\text{Pu}$  and  $^{238}\text{Pu}$ . The red lines are fits of the experimental data with two-tailed Bortels functions.

## RESULTS AND DISCUSSION

To obtain the energy spectrum several data postprocessing steps are necessary. The raw data contains a set of voltage pulse records with pulse height proportional to the energy deposited in the absorber. The first step involves performing several cuts with respect to timestamp, pre-trigger baseline voltage and pulse maximum position to eliminate records with baseline jumps, pulse pileup and other non-pulse events. Second, an energy peak is selected to calculate an average pulse, which, together with the initial noise record, is used to compute the Wiener optimal filter. Third, drift correction is applied to the optimal filtered data set by smoothing the timestamp spectrum of a selected peak and subtracting the smoothed results. Fourth, the spectrum is calibrated by using the *Q*-values for  $^{239}\text{Pu}$  and  $^{238}\text{Pu}$  as fix points and interpolating the pulse height with a low-order polynomial.

We were able to detect three distinct energy peaks, corresponding to the decays of  $^{238}\text{Pu}$ ,  $^{239}\text{Pu}$  and  $^{240}\text{Pu}$  at 5593.2 keV, 5244.5 keV and 5255.82 keV respectively. An example spectrum recorded over a timespan of ~12h is shown in Figure 2. Events corresponding to the alpha decay of  $^{242}\text{Pu}$  were also detected but only amount to about 5-10 counts and are not shown here. The  $^{239}\text{Pu}$  and  $^{240}\text{Pu}$  lines are clearly separated with almost no overlap between them. The fwhm of each peak is about 1keV - one order of magnitude better than typical achieved by  $\alpha$ -spectroscopy.

The isotopic composition with respect to  $^{238}\text{Pu}$ ,  $^{239}\text{Pu}$ ,  $^{240}\text{Pu}$  and  $^{242}\text{Pu}$  was determined by least-square fits of the spectra with two-tailed Bortels functions [Bortels1987]. This allows us to account

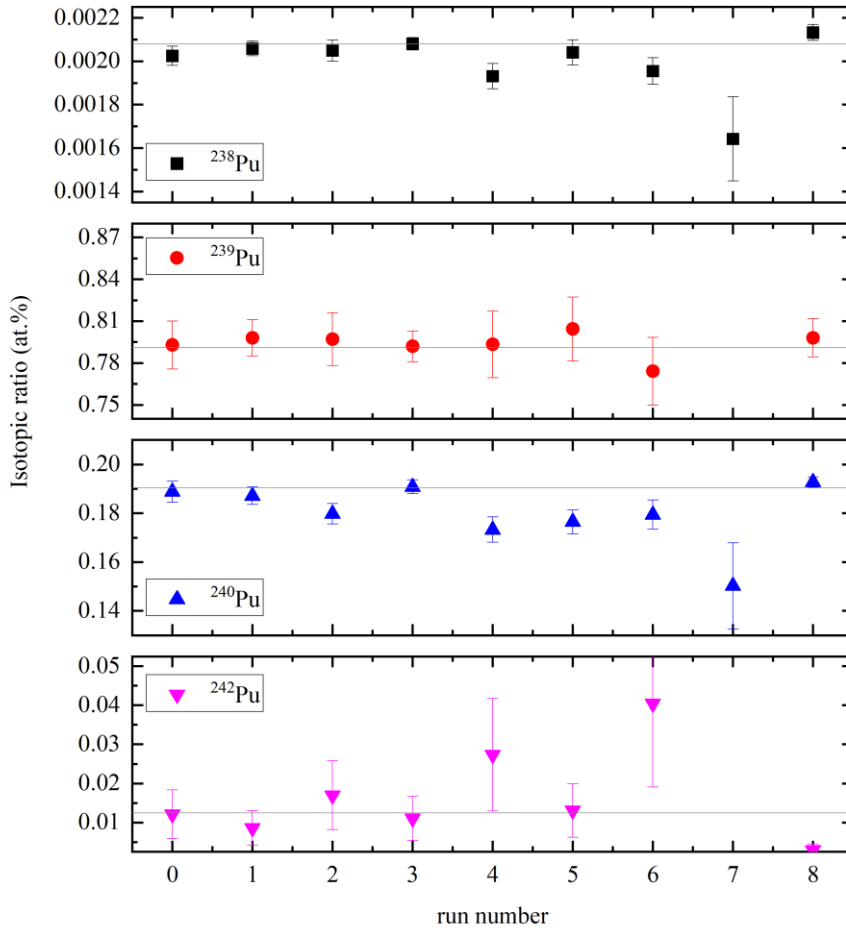


Figure 3: Isotopic ratios of  $^{238}\text{Pu}$ ,  $^{239}\text{Pu}$ ,  $^{240}\text{Pu}$ , and  $^{242}\text{Pu}$  of sample 1B for several consecutive runs. The grey horizontal lines mark the decay corrected catalogue reference values [NBL2002].

for potential incursions of the low energy tails of the  $^{240}\text{Pu}$  peak into the neighboring  $^{239}\text{Pu}$  peak, that would not be considered by simply integrating the area under each peak. The amplitude of the Bortels fits is then proportional to the fraction under consideration of the half-life of each isotope. Results of 9 consecutive  $\sim 12\text{h}$  measurements of sample 1B are shown in Figure 2. Overall, the results are scattered around the reference values with few outliers. Note that in some situations pulse records were discarded due to pre-trigger baseline jumps that cannot be drift corrected by our current algorithms. This results in fewer pulses being counted, an increase in the statistical uncertainty and larger relative overlap between the  $^{239}\text{Pu}$  and  $^{240}\text{Pu}$  lines – which is the main source of the uncertainty of the respective isotopics (e. g. run number 7 in Figure 3). Data analysis algorithms are currently in development to better utilize the collected data. As discussed in [Hoover2015] variations in the sample preparation (mechanical kneading) also affect the peak width.

We summarize our results in Table 1, showing the averaged isotopic composition weighted by the inverse uncertainty of all three CRM 137A samples and the reference values obtained from mass spectroscopy.  $^{241}\text{Pu}$  does not have a significant alpha decay channel and mainly undergoes beta decay to  $^{241}\text{Am}$  ( $\sim 20\text{keV}$ ), which is below the detectable energy threshold for a detector/absorber

design optimized for ~5MeV energies. The isotopic composition of  $^{238}\text{Pu}$ ,  $^{239}\text{Pu}$  determined from the DES spectral analysis agree with the decay corrected reference values within the  $1\sigma$  statistical uncertainties. Note that the DES results for  $^{242}\text{Pu}$  have to be taken with caution, due to the low number of counts associated with this isotope.

*Table 1: Isotopic composition (at%) and uncertainties of  $^{238}\text{Pu}$ ,  $^{239}\text{Pu}$ ,  $^{240}\text{Pu}$  and  $^{242}\text{Pu}$  in three DES samples (1A, 1B, 1C) and decay corrected reference values for CRM 137 taken from [NBL2002]. Note that the values for  $^{241}\text{Pu}$  marked with \* were fixed to the reference values, since  $^{241}\text{Pu}$  cannot be detected with DES.*

	$^{238}\text{Pu}$ (at%)	$^{239}\text{Pu}$	$^{240}\text{Pu}$	$^{242}\text{Pu}$	$^{241}\text{Pu}$
1A	0.2037 (54)	79.5 (21)	18.08 (50)	1.9 (10)	0.414*
1B	0.2021 (48)	78.9 (19)	18.27 (45)	4.0 (23)	0.414*
1C	0.2054 (56)	78.5 (21)	18.77 (54)	2.3 (12)	0.414*
CRM 137	0.208 (5)	79.105 (22)	19.038 (22)	1.235 (4)	0.414 (4)

## SUMMARY

We performed DES on dried solutions of CRM 137A incorporated into a gold absorber by mechanical kneading. DES has several advantages over conventional methods like mass spectrometry and  $\alpha$ -spectroscopy. Besides the simple sample preparation, DES offers energy resolutions of about 1keV at ~5MeV and can efficiently analyze small amounts (~1Bq) of nuclear material. Unlike mass spectroscopy, DES is unaffected by isobaric interferences such as  $^{238}\text{Pu}/^{238}\text{U}$  and  $^{241}\text{Pu}/^{241}\text{Am}$  and allows for the recovery of the measured nuclear material for potential analysis via other techniques. The spectra present a single energy peak for each Pu isotope, from which the isotopic composition of three samples were extracted. Our results are in good agreement with catalogue values for CRM 137. With further improvements regarding data analysis and easier instrumentation on the way, we believe that the DES method is an important tool in safeguards and nuclear forensics.

## ACKNOWLEDGEMENT

Funding of this project was provided by the US Department of Energy Office of Nuclear Energy.

## REFERENCES

- [Koehler2013] K. E. Koehler *et al.*, “Q Spectroscopy With Superconducting Sensor Microcalorimeters.” *IEEE Transactions in Nuclear Science* 60 (2013): 624–629.
- [Hoover2015] A. S. Hoover *et al.*, “Measurement of the  $^{240}\text{Pu}/^{239}\text{Pu}$  Mass Ratio Using a Transition-Edge-Sensor Microcalorimeter for Total Decay Energy Spectroscopy.” *Analytical Chemistry* 87 (2015): 3996-4000.
- [Irwin2005] K. D. Irwin and G. C. Hilton, “Transition-Edge Sensors”, In *Cryogenic Particle Detection*; C. Enss, Ed.; *Topics in applied Physics* 99 (2015): 63-149.

[Bortels1987] G. Bortels and P. Collaers, “Analytical Function for Fitting Peaks in Alpha-Particle Spectra from Si Detectors.” *Applied Radiation and Isotopes* 38 (1987): 831-837.

[NBL2002] *Certified Reference Material CATALOG* (2002): 16.